Ambient Gas Density Effects on Droplet Diameter and Velocity in a Transient Diesel Fuel Spray

J.Y.Koo and J.K.Martin

Engine Research Center
University of Wisconsin-Madison
1500 Johnson Drive
Madison, WI 53706
U.S.A.

ABSTRACT

Simultaneous droplet sizes and velocities have been measured using a Phase/Doppler Particle Analyzer (PDPA) in a transient diesel fuel spray. Investigated are the effects of injection into ambient gas of differing density and pressure.

Increases in $\rho g / \rho l$ resulted in greatly decelerated and extended fuel sprays at the measurement location (x/D=250). Droplet sizes tended to be relatively constant at the higher $\rho g / \rho l$, in contrast to the lower $\rho g / \rho l$, where droplet sizes continuously decreased. At the edge of the spray, a mixing region caused a nonuniform droplet/velocity correlation.

INTRODUCTION

Detailed knowledge of the structure of transient diesel fuel sprays is a prerequisite to the understanding and accurate prediction of diesel combustion behavior. Although there have been many experimental and theoretical studies of fuel sprays, most of these studies have been carried out for steady, or non-engine like conditions. Recent experimentation suggests that important physical behavior arising from the transient nature of real diesel sprays may be missed in studies of steady-state sprays [1, 2]. Thus there remains a need for detailed information about droplet size and velocity distributions for transient diesel sprays, in particular at pressures and temperatures that are typical of actual engine conditions. Presented here are results from experiments designed to show the effects of variations in ambient-gas density on the transient fuel spray behavior. Experiments were performed for a range of gas-to-liquid density ratios from 1.37×10^{-3} to 29.2×10^{-3}, under isothermal conditions (room temperature), simulating the range of density ratios encountered for free-atmospheric sprays to diesel engine injection.

EXPERIMENTAL DESCRIPTION

Experimental Apparatus

The primary diagnostic used in this study for the measurement of droplet sizes and velocities is an Aerometrics Phase Doppler/Particle Analyzer (PDPA). As has been discussed previously, transient diesel sprays are very dense sprays which require much care in the use of the instrument [2]. Because of practical limitations of the instrument and the complex nature and density of these sprays, it is unlikely that the accurate measurement of flux quantities can be accomplished. These quantities are not reported here. In a prior study, measurements were made in regions of the spray where the drop-size range of the instrument was exceeded at a single instrument setting, which produced results that were typical of a subgroup of droplet sizes [2]. To avoid any ambiguities regarding the quantities reported here, the measurements were made in regions of the spray where the largest drops were measured, with a lower limit of 2.0-2.3 μm in diameter.

A comment must be made regarding validation of drop-size measurements and apparent conditional sampling. Because the PDPA requires a single, nearly-spherical droplet to be present in the measurement volume to make a valid size measurement, dense diesel fuel-sprays have regions where the above criteria are frequently not meet. Thus it is possible that the group of droplets that produce valid size measurements are not characteristic of the true ensemble of drops and other liquid present.

Shown in Fig. 1 is a schematic of the experimental apparatus. For all the data to be presented, the x-axis is assumed to be coincident with the central axis of the injector. Each velocity and size measurement is coupled with a measurement of pump-shaft rotational position, which allows for phase-averaging. Details of the spray chamber can be found in Ref. [3].

Experimental Procedures

To investigate the effects of ambient gas density on injection, four different gas pressures were used. These conditions are shown in Table 1, with a calculation of the gas-to-liquid density ratio. Typical diesel conditions have a $\rho g / \rho l$ range from 15×10^{-3} to 30×10^{-3} [4]. In all cases the gas was isothermal at room temperature, with injection into quiescent or nearly-quiescent gas.

Table 1 Ambient gas state

Pgas (MPa)	Gas Composition	$\rho_g / \rho_l \times 10^3$
0.10	N2 (80%) Air (20%)	1.37
0.47	N2 (100%)	6.00
1.34	N2 (100%)	18.1
2.17	N2 (100%)	29.2

Reported are the phase- or ensemble-average of the velocity, U, defined

$$\bar{U}(\theta, \Delta\theta) = \frac{1}{N_t} \sum_{i=1}^{N_c} \sum_{j=1}^{N_j} U_{ij}(\theta \pm \frac{\Delta\theta}{2}) \qquad (1)$$

and an rms velocity, Urms, defined

$$U_{rms}(\bar{\theta}, \Delta\theta) = \left[\frac{1}{N_t} \sum_{i=1}^{N_c} \sum_{j=1}^{N_i} u_{ij}^2 (\bar{\theta} \pm \frac{\Delta\theta}{2}) \right]^{\frac{1}{2}} \quad (2)$$

where $u_{ij} = U_{ij} - U$

Note that these quantities were calculated for the entire range of droplet sizes measured. There may be significant differences in the behavior of drops in any particular size range. Similarly, the actual gas-phase turbulence intensity may be much different from that calculated here. To characterize the drop sizes both the Sauter Mean Diameter, SMD, defined

$$d_{32}(\bar{\theta}, \Delta\theta) = \frac{\sum_{i=1}^{N_c} \sum_{j=1}^{N_i} d_{ij}^3 (\bar{\theta} \pm \frac{\Delta\theta}{2})}{\sum_{i=1}^{N_c} \sum_{j=1}^{N_i} d_{ij}^2 (\bar{\theta} \pm \frac{\Delta\theta}{2})} \quad (3)$$

and the arithmetic mean diameter, AMD, defined

$$d_{10}(\bar{\theta}, \Delta\theta) = \frac{\sum_{i=1}^{N_c} \sum_{j=1}^{N_i} d_{ij} (\bar{\theta} \pm \frac{\Delta\theta}{2})}{\sum_{i=1}^{N_c} \sum_{j=1}^{N_i}} \quad (4)$$

are presented.

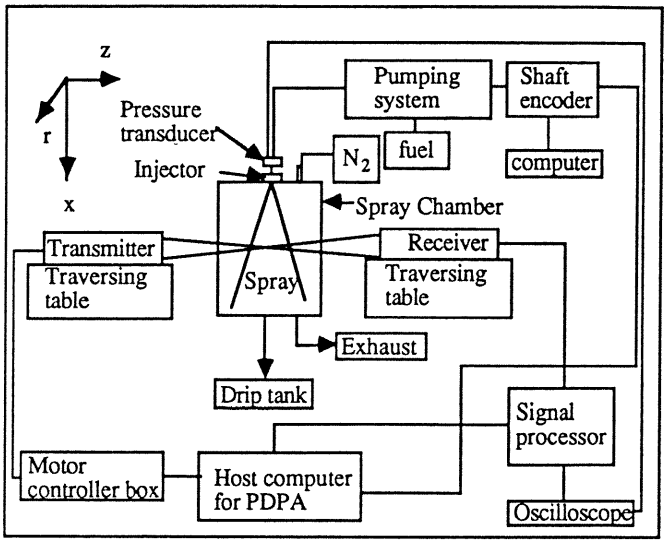

Fig.1 Schematic diagram of experimental apparatus

VELOCITY/DIAMETER RESULTS

Characteristics of the single-hole nozzle, pump operation, and instrument settings are given in Fig. 2. The injected fuel quantity was held constant for all of the measurements to be presented.

First, results from velocity measurements directly on the axis of the spray at a position 60 mm from the injector tip are presented. Figure 3 shows the results for the range of ambient gas pressures investigated. It is clear from Fig. 3 that the ambient gas density has strong effects both on the structure and transient behavior of this diesel fuel spray. As expected, the magnitudes of the velocities are greatly affected by the ambient gas density. In all cases we observe that the droplets that reach the measurement volume first are over-

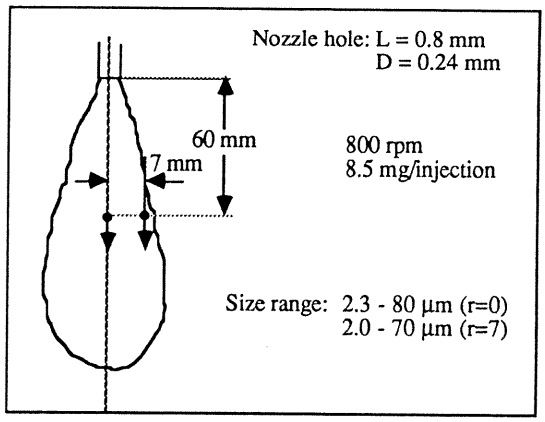

Fig.2 Measurement positions and conditions

taken by the droplets that are injected after them. However, a increase in ρ_g / ρ_l results in much longer periods during the injection at which this phenomenon occurs. This results in part because of the higher gas densities, which effectively extend the duration of the spray at positions in the far-field of the spray. This temporal extension of the fuel spray as a result of increases in ρ_g / ρ_l is evident in all of the data to follow.

The rms velocities exhibited in Fig. 3 range from peak values of 20 m/s at the lowest gas pressure to 10 m/s at the highest gas pressure. Thus, the rms intensity (Urms/U) is greatly increased as the gas density is increased, probably as a result of much larger gas turbulence at the higher gas densities.

Droplet diameter measurements for the same location are presented in Fig. 4. These results are best interpreted if the spray passing this position is divided into three parts consisting of the tip, the quasi-steady region, and the tail. The drop-size characteristics at the tip of the spray consist of those data reaching the measurement volume first after the start of injection. For the lowest ambient gas pressure condition the drops in the tip of the spray are larger (SMD=50 μm) than at any other time during the spray. This is in contrast to the other ambient gas pressure conditions where the droplets in the tip of the spray tend to be smaller than those that follow them. Droplet breakup right in the spray tip is probably the cause of this. Table 2 lists the relative droplet velocity (Vdroplet - Vgas) needed for a droplet to have a droplet Weber number equal to a critical value of 12. Pilch and Erdman [5] claim this is the minimum value necessary for a droplet to undergo bag breakup.

Table 2 Relative velocity for $We_{cr} = 12$

Diameter (μm)	$\rho_g / \rho_l \times 10^3$	Vdroplet-Vgas (m/s)
10		171
30	1.37	99
60		70
10		82
30	6.0	47
60		33
10		47
30	18.1	27
60		19
10		37
30	29.2	22
60		15

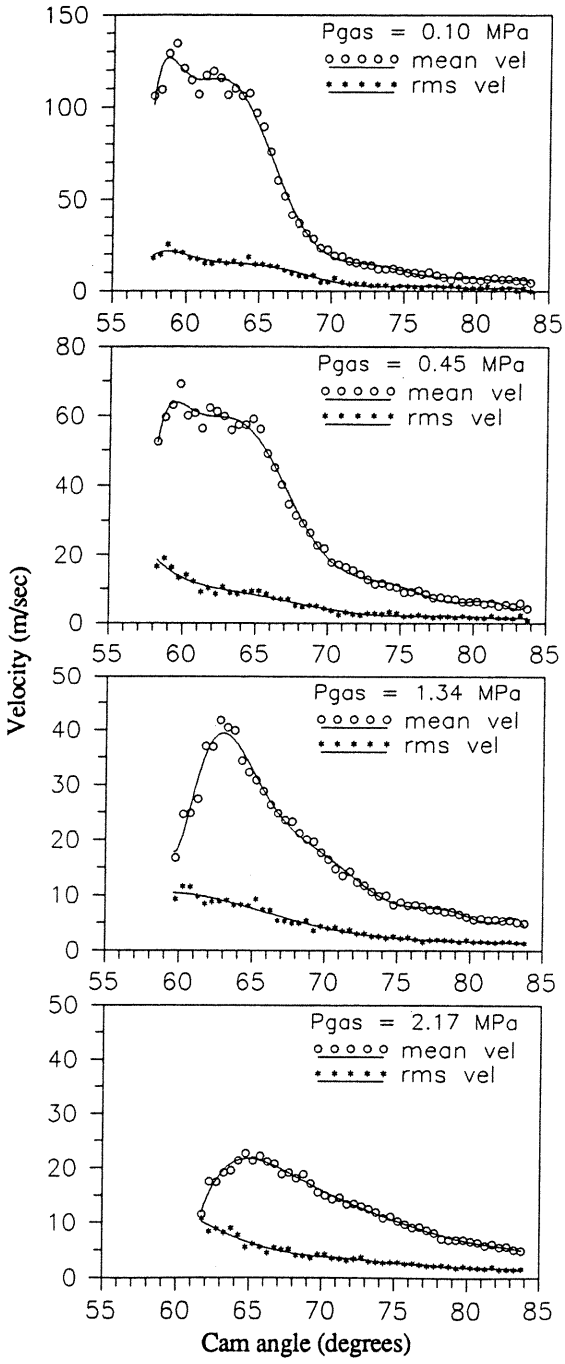

Fig.3 Phase - averaged mean and rms - velocities for different gas pressures at x=60 mm and r=0 mm

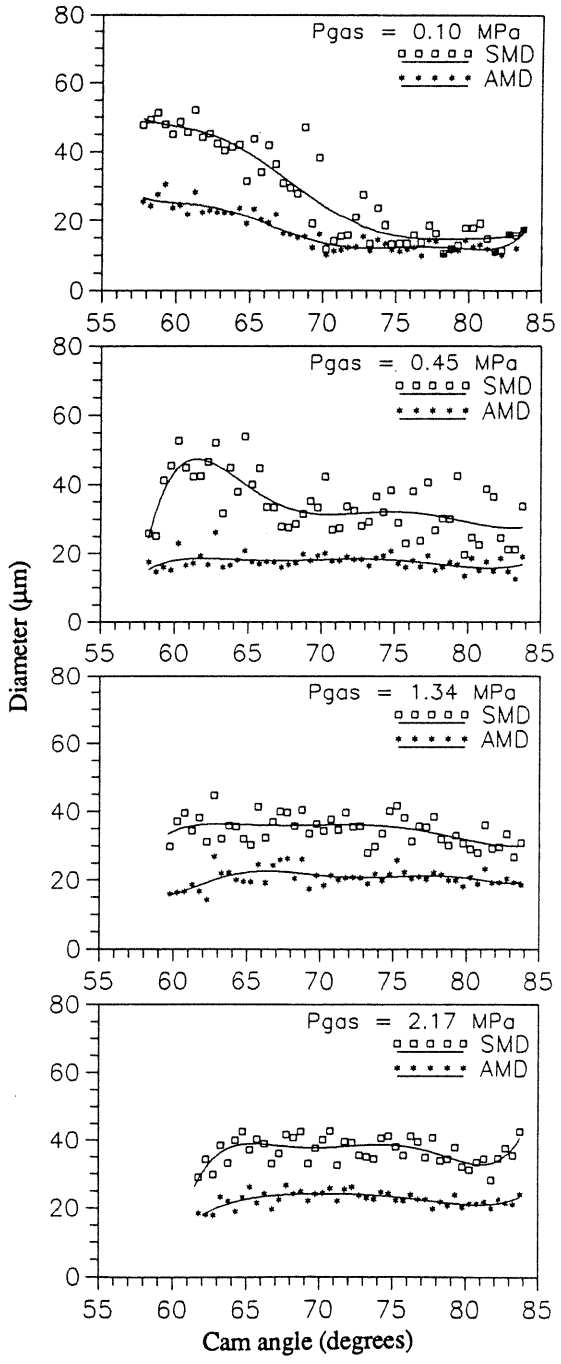

Fig.4 Phase - averaged SMD and AMD for different gas pressures at x=60 mm and r=0

At the lower ρ_g / ρ_l, the droplets decrease in size throughout the quasi-steady portion of the spray, again in contrast to the higher ρ_g / ρ_l conditions where the droplet sizes are relatively constant during this period. The V_{rel} listed in Table 2 seem to explain this result. For example, the droplets of a size equal to the SMD found at the lower pressure conditions will likely be unstable. On the other hand, the We_{cr} for a droplet of a size equal to the SMD at the higher gas pressure conditions requires a relative velocity larger than that observed in the data. Thus we would expect relatively stable drops through this region at these conditions.

Finally, at the tail of the spray, the atmospheric pressure condition results in the smallest droplets (SMD<20 μm). This may result from a spatial dependence in droplet size at the end of the spray because of differences in the momentum-to-drag ratio of droplets of different sizes [2,6]. However, at the highest gas pressure condition, the tail of the spray contains the largest droplets found for this condition with the SMD increasing to 45 μm from 30 μm at the spray head. This may be a result of drop coalescence.

The effects of changes in ρ_g / ρ_l on the ensemble-mean and rms velocities at the edge of the fuel spray are depicted in Fig. 5. For the lowest density ratio, the mean velocity at

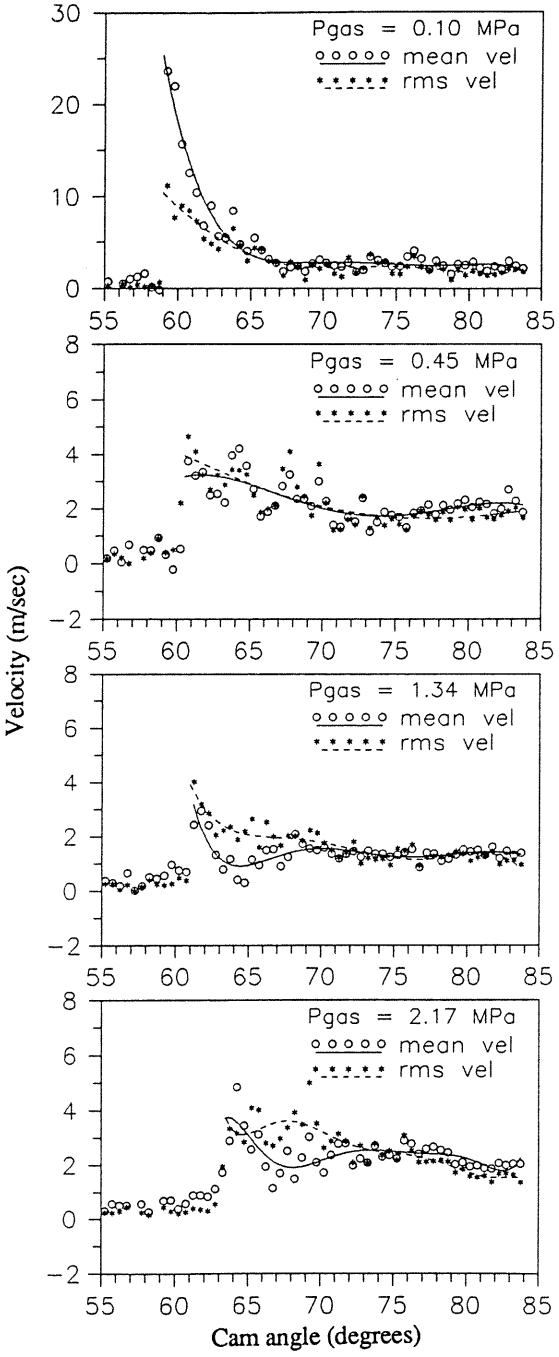

Fig.5 Phase - averaged mean and rms - velocities for different gas pressures at x=60 mm and r=7 mm

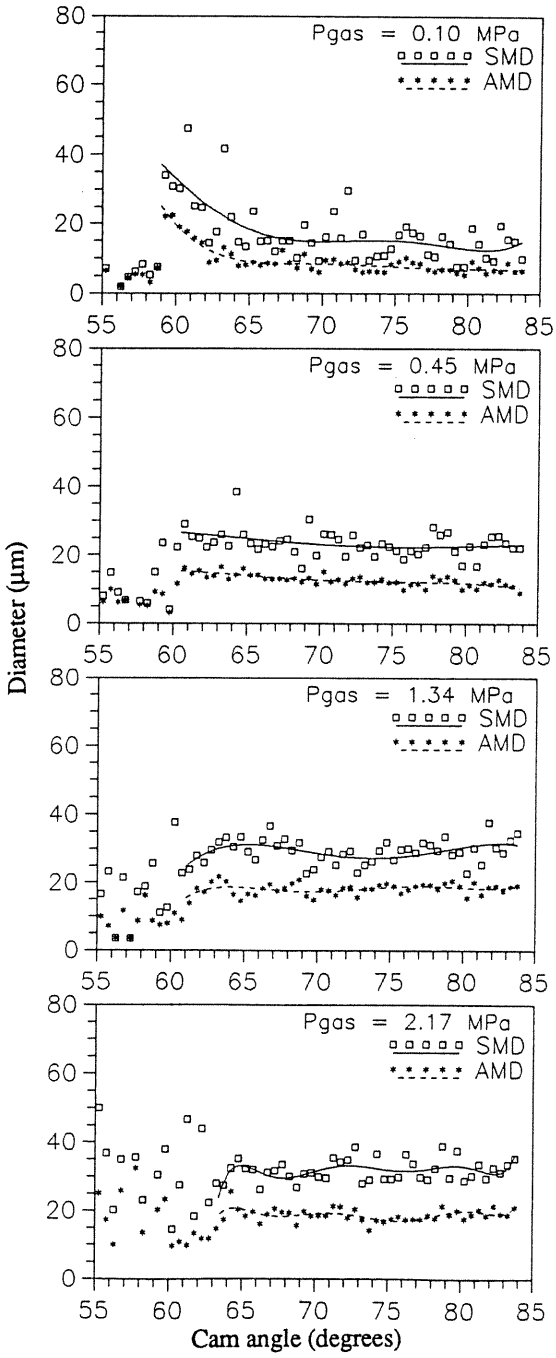

Fig.6 Phase - averaged SMD and AMD for different gas pressures at x=60 mm and r=7 mm

the head of the spray is approximately 25 m/s, which quickly falls through the rest of the spray. The initial rms velocities are also large, with values as high as 10 m/s at the tip. The transient behavior indicates that the spray angle is a function of time here, which has also been observed in high-speed movies of this condition. As the density of the ambient gas is increased, again the peak velocities are reduced. The velocity does continue to change throughout the injection event, however. Note that in all of the higher gas density cases, the rms velocities are similar in magnitude to the mean, indicating very high values of the rms intensity at this position.

Corresponding droplet diameters shown in Fig. 6 exhibit results similar to those found on the axis of the spray, although the droplet sizes tend to be smaller by approximately 20 percent.

Using ensemble or phase-averaged results for these fuel sprays can produce a picture of the spray structure which is misleading. For example, mean velocities measured at the edge of the fuel spray at the highest ambient gas density condition (Fig. 5) were 4 m/s compared to the 20 m/s observed at the axis of the spray (Fig. 3). However, individual measurements displayed in Fig. 7a reveal maximum positive velocities of 15 m/s at the spray edge, as well

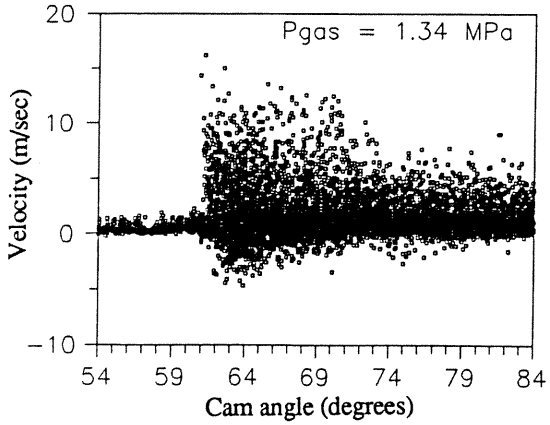

Fig.7a Crank-angle resolved droplet velocities at x=60 mm and r=7 mm

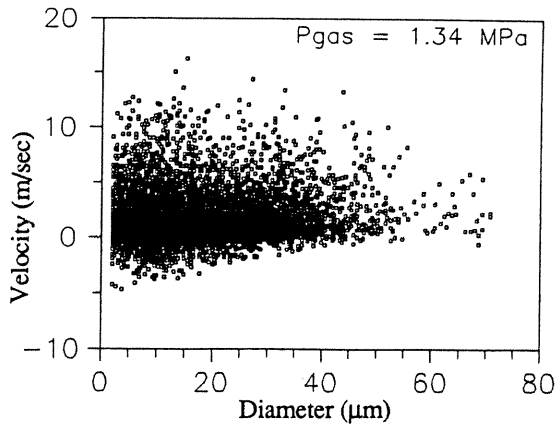

Fig.7b Crank-angle resolved droplet velocity and size correlations at x=60 mm and r=7 mm

as negative velocities of almost 5 m/s. This range of velocities occurs because of vortices formed in the shear layer observed to occur at the edge of the spray.

In Fig. 7b the same velocity data are plotted with corresponding diameter measurements. Droplets larger than 40 μm tend to have only positive velocities, thus indicating that these droplets may be slowed by the rotating gas flow, but do not follow it. The smallest droplets have the largest negative velocities, and it appears that the peak magnitude of negative velocity is inversely proportional to droplet diameter.

Using the velocity/diameter measurements, it is possible to determine a tip penetration rate. These data are presented in Fig. 8. The spray tip was assumed to have arrived at the measurement volume of the PDPA at the time of the first valid measurement after the needle has begun to move. As expected, the greater the ambient gas density, the slower the tip penetration rate. At atmospheric pressure, the tip penetration rate was nearly constant after the spray tip had travelled 20 mm from the nozzle throughout the rest of injection. Further, nozzle hole size had very little effect on the tip penetration rate for injection into atmospheric pressure, as the 240 μm nozzle and 400 μm nozzle had nearly identical penetration rates. This is in contrast to injection into the higher gas densities where the larger diameter hole produced higher penetration rates. For all conditions, the initial penetration rate continuously increased, similar to results observed by Hiroyasu [7]. An inflection point is observed in the penetration/time data at 20 mm from the nozzle, after which the penetration rate is reduced approximately with the root of the liquid-to-gas density ratio.

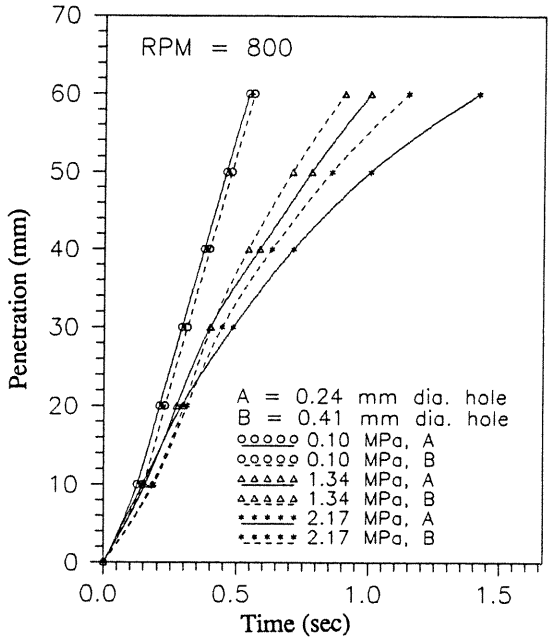

Fig.8 Spray penetration determined from velocity measurements for different gas pressures

SUMMARY

For this investigation of the effects of $\rho g / \rho l$ on droplet size and velocity characteristics in a transient diesel spray at x/D=250 (x=60 mm):

1. An increase in $\rho g / \rho l$ results in increases in the effective duration of the spray at all points in the far-field of the spray. This results, for example, in extension of the period at the beginning of the spray when first injected droplets are overtaken by droplets that are injected after them.

2. In general the droplet sizes tend to be relatively stable at the $\rho g / \rho l$ typical of direct injection. This is in contrast to the lower $\rho g / \rho l$, where the droplet Weber numbers are sufficiently large at x/D=250 that droplet breakup occurs throughout the spray event.

3. Evidence of vortices formed at the edge of the spray at the higher $\rho g / \rho l$ resulted in a highly turbulent flow with droplet size stratification.

4. Using the velocity measurements, tip penetration rates showed characteristics that were similar to previous investigations.

ACKNOWLEDGEMENTS - General Motors Corp. is acknowledged for the donation of the experimental injector used in this study. Support from Kia Motors Corporation for this study is acknowledged. Partial support for this work came from funding administered by the Army Research Office for the Engine Research Center.

REFERENCES

1. Yule, A.J. and Aval, S.M., "A Technique for Velocity Measurements in Diesel Sprays," Combustion and Flame, Vol. 77, pp. 385-394, 1989.

2. Koo, J.Y. and Martin, J.K., "Droplet Sizes and Velocities in a Transient Diesel Fuel Spray," SAE Paper No. 900397, 1990.

3. Bower, G.R., Chang, S.K., Corradini, M.L., El-Beshbeeshy, M., Martin, J.K., and Krueger, J., "Physical Mechanisms for Atomization of a Jet Spray: A Comparison of Models and Experiments, SAE Trans., Vol. 97, SAE Paper No. 881318, 1988.

4. Bracco, F.V., "Modeling of Engine Sprays," in Engine Combustion Analysis: New Approaches, SAE Publication P-156, SAE Paper No. 850394, 1985.

5. Pilch, M. and Erdman, C.A., "Use of Breakup Time Data and Velocity History Data to Predict the Maximum Size of Stable Fragments for Acceleration-Induced Breakup of a Liquid Drop," Int. J. Multiphase Flow, Vol. 13, No. 6, pp. 741-757, 1987.

6. Hardalupas, Y., Taylor, A.M.K.P., and Whitelaw, J.H., "Characteristics of Unsteady Sprays," Report FS/89/21, Mech, Engrg. Dept., Imperial College, 1989.

7. Hiroyasu, H., "Diesel Engine Combustion and Its Modeling," Proc. of the Int. Symp. on Diagnostics of Modeling and Combustion in Reciprocating Engines, COMODIA 85, Tokyo, 1985.